

Synthesis and DFT calculation on novel derivatives of Bis (indolyl) methanes



Maryam Zarandi*, Alireza Salimi Beni

Department of Chemistry, Yasouj University, Yasouj, 75918-74831, Iran

ARTICLE INFO

Article history:

Received 25 December 2015

Received in revised form

10 April 2016

Accepted 25 April 2016

Available online 29 April 2016

Keywords:

Bis (indolyl) methane

Aldehyde

Synthesis

Theory

ABSTRACT

Bis (indolyl) methane derivatives are an important class of biomolecules and heterocyclic scaffold of organic compounds. To extension novel Bis (indolyl) methane derivatives, two new aldehydes have been applied. In order to structural investigation, the optimized geometry, total energy, potential energy surface and vibrational wavenumbers of Bis (indolyl) methanes have been determined using DFT/B3LYP method with 6-31G (d) basis set. A complete vibrational assignment is provided for the observed IR spectra of Bis (indolyl) methanes. These methods are proposed as a tool to be applied in the structural characterization of Bis (indolyl) methanes. The isotropic chemical shift computed by ¹H and ¹³C NMR chemical shifts of the Bis (indolyl) methanes, calculated using the GIAO method, shows good agreement with experimental observations. The calculated HOMO and LUMO with frontier orbital gap are presented in order to predict antibacterial properties.

© 2016 Elsevier B.V. All rights reserved.

1. Introduction

In recent years, the synthesis of bis heterocycles with an appropriate linker has attracted considerable academic attention due to their special pharmacological properties. Versatile Bis (indolyl) methanes by symmetrical or unsymmetrical structures contain aryl/alkyl groups are reported to be biologically important [1–4]. Bis (indolyl) methanes as cruciferous substances promote estrogen metabolism and induce apoptosis in human cancer cells [5]. Also these compounds applied in colorimetric sensors and chromogenic sensors [6]. Synthesis of new Bis (indolyl) methanes derivatives is desirable due to their wide occurrence as natural products and various biological activities. The simple and the straightforward protocol for the synthesis of Bis (indolyl) methanes is reaction of 1H-indole with aldehydes or ketones produces azafulvenium salts that react further with a second 1H-indole molecule to form bis(indol-3-yl)methanes [7]. Various synthetic methods for preparation of Bis (indolyl) alkane derivatives have been reported in the literature by reaction of indole with various aldehydes and ketones [8–16].

The substituted new aldehyde derivatives are very promising materials for future colorimetric sensors and chromogenic sensors

applications. The inclusion of substituents new aldehydes leads to the variation of charge distribution in the molecule, and consequently affects the structural, electronic and vibrational parameters. One of the interesting field of academic research is synthesis and theoretical investigation of structural parameter of different organic and inorganic compound [17–19]. In order to importance and vide range application, however, reports on the structure parameters and spectroscopic properties of Bis (indolyl) methanes are interesting and demanding [20,21]. Therefore, in the present paper we continue our research program on deep investigation of organic compound [22–24]. By consideration of versatile application of Bis (indolyl) methanes such as biological, corrosion inhibitor, sensor and so on [25,26]; it has been undertaken to synthesis and the theoretical approach of geometrical parameters, vibrational frequencies, molecular electrostatic potential, NBO analyses and HOMO, LUMO of two new derivatives of Bis (indolyl) methanes.

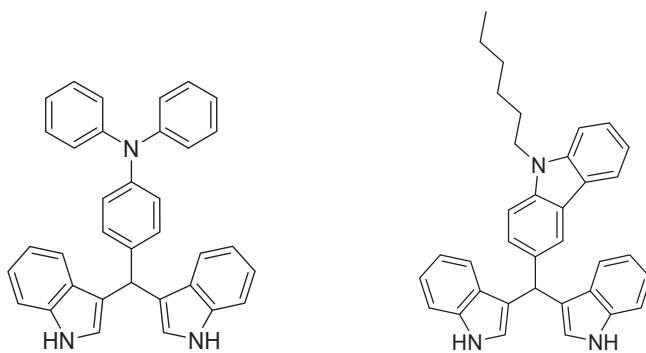
2. Experimental

2.1. Chemicals and apparatus

All solvents and other chemicals were reagent grade and used without further purification. All chemicals were purchased from Merck and Sigma–Aldrich. Melting points were measured on an electrothermal KSB1N apparatus. The ¹H NMR (400 MHz) and ¹³C NMR (100 MHz) were run on Bruker AvanceDPX-400 spectrometer

* Corresponding author.

E-mail address: maryam.zarandi88@gmail.com (M. Zarandi).

**Scheme 1.** Chemical structure of BIM1 and BIM2.

in DMSO-*d*₆ solvent, with tetramethylsilane (TMS) as the standard and *J* values are given in Hz. 2. Diameter of NMR tube was 5 mm. The software that used for interpretation of peaks was ACD/NMR Processor Academic Edition. FT-IR spectra were recorded in the matrix of KBr with JASCO FT-IR-680 plus spectrometer. 6. The program name of used for FT-IR analysis was spectra manager and scale factors was 0.95. Reaction monitoring was accomplished by TLC on silica gel polygram SILG/UV 254 plates. Mass spectra of the products were obtained with a HP (Agilent technologies) 5937 Mass Selective Detector.

2.1.1. Preparation of alumina sulfuric acid

In a 500 mL flask equipped by a dropping funnel and a gas inlet tube for conducting HCl gas over adsorbing solution e.g. water. Acidic Alumina (51 g, 510 mmol) was charged in the flask and

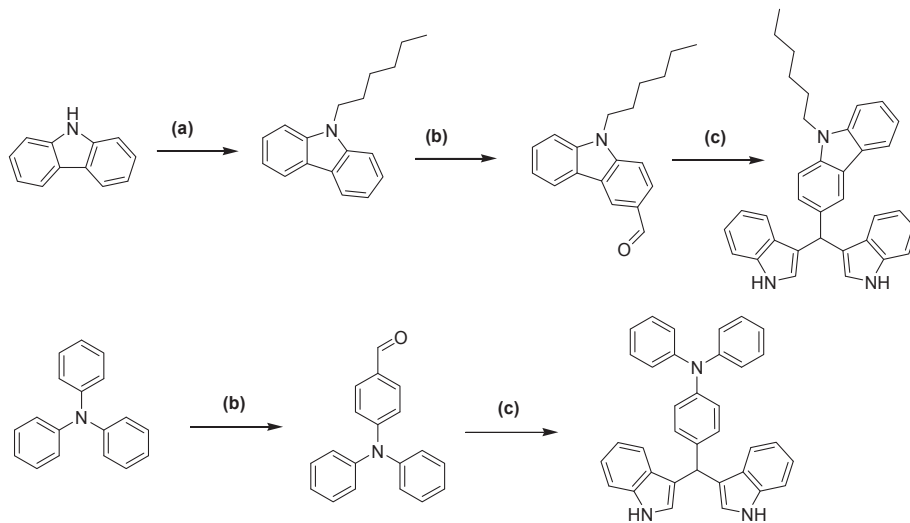
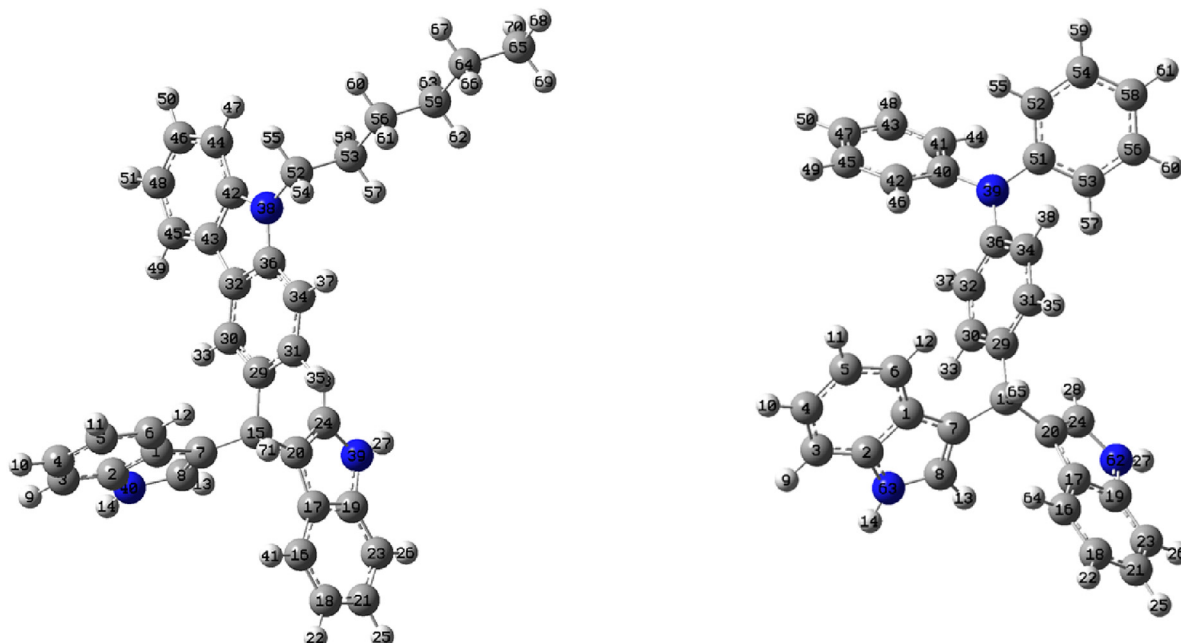
**Scheme 2.** Synthetic routes of BIM1 and BIM2 (a) 1-Bromohexane, NaOH, DMSO, 110 °C, overnight (b) POCl₃, DMF, 95 °C, overnight (c) Indole, Alumina sulphuric acid, Ethanol, 50 °C, 3 h.**Fig. 1.** The optimized structure and numbering of the tautomer of BIM1 and BIM2.

Table 1

Computed geometrical parameter for the ground state of BIM1 and BIM2 at DFT method using 6–31 g (d) basis set.

Geometrical parameter	BIM2	Geometrical parameter	BIM1
Bond length(r)		Bond length(r)	
C1–C2	1.4223	C1–C2	1.4223
C1–C6	1.4058	C1–C6	1.4058
C1–C7	1.4452	C1–C7	1.4453
C7–C8	1.3724	C7–C8	1.3724
C7–C15	1.5156	C7–C15	1.5155
C15–C20	1.5172	C15–C20	1.5172
C16–C17	1.4062	C17–C20	1.4459
C17–C19	1.4224	C20–C24	1.3725
C17–C20	1.4460	C16–C17	1.4061
C20–C24	1.3724	C15–C29	1.5330
C15–C29	1.5310	C2–N40	1.3801
C29–C30	1.4003	C8–N40	1.3834
C29–C31	1.4006	C19–N39	1.3799
C30–C32	1.3931	C24–N39	1.3835
C31–C34	1.3928	C36–N38	1.3916
C32–C36	1.4035	C42–N38	1.3910
C34–C36	1.4035	C52–N38	1.4526
C40–C41	1.4048	C6–H12	1.0866
C40–C42	1.4046	C8–H13	1.0804
C51–C52	1.4047	C15–H71	1.1016
C51–C53	1.4047	C16–H41	1.0865
C2–N63	1.3802	C24–H28	1.0804
C8–N63	1.3831	C52–H54	1.0962
C19–N62	1.3800	C52–H55	1.0964
C24–N62	1.3833	C53–H57	1.0981
C36–N39	1.4226	C53–H58	1.0981
C40–N39	1.4215	N39–H27	1.0077
C51–N39	1.4208	N40–H14	1.0076
C6–H12	1.0867	C1C7C15	126.0792
C8–H13	1.0804	C8C7C15	127.6219
C16–H64	1.0865	C17C20C15	126.3108
C24–H28	1.0804	C24C20C15	127.4429
C30–H33	1.0865	C7C15H71	106.4305
C31–H35	1.0881	C1C6H12	120.3887
C32–H37	1.0856	C7C15C20	112.6385
C34–H38	1.0856	C20C15H71	106.4686
C41–H44	1.0854	C29C15H71	106.0786
C42–H46	1.0852	C7C8H13	129.3143
C52–H55	1.0853	C20C24H28	129.3029
C53–H57	1.0853	C6C1C7C15	0.43766
N62–H27	1.0077	C1C7C15H71	48.68336
N63–H14	1.0077	C17C20C15H71	48.61180
Bond Angles (°)		H13C8C7C15	1.04043
C6C1C7	134.0015	H28C24C20C15	−0.13790
C1C6H12	120.4212	C31C29C15H71	96.92431
C15C7C8	127.6763	C30C29C15H71	−156.24673
C7C8H13	129.3136	C42N38C52H55	148.68133
H13C8N63	120.6473	C36N38C52H54	−33.12108
C8N63H14	125.1138	H47C44C42N38	0.92750
C2N63H14	125.5078	H37C34C36N38	−1.00636
C7C15C20	112.7629	—	—
C7C15H65	106.5615	—	—
C29C15H65	106.0691	—	—
C15C20C24	127.5367	—	—
C15C20C17	126.1983	—	—
N63C8H13	120.6473	—	—
C36N39C51	119.9251	—	—
C36N39C40	119.9464	—	—
C40N39C51	120.1187	—	—
H37C32C36	119.4159	—	—
H38C34C36	119.5268	—	—
H44C41C40	119.4125	—	—
H46C42C40	119.4538	—	—
H55C52C51	119.3758	—	—
H57C53C51	119.3193	—	—
C15C7C8H13	1.2324	—	—
C7C1C6H12	1.1925	—	—
C1C7C15H65	49.0590	—	—
C15C29C30H33	2.2160	—	—
C15C20C24H28	−0.2531	—	—
C17C20C15H65	−23.0962	—	—
C32C36N39C40	42.7369	—	—

Table 1 (continued)

Geometrical parameter	BIM2	Geometrical parameter	BIM1
C34C36N39C51	42.0468	—	—
C34C36N39C40	−136.8171	—	—
N39C51C52H55	0.4099	—	—
N39C41C40N39	0.3545	—	—

chlorosulfonic acid (14 mL, 210 mmol) was added drop wise over a period of 1 h at room temperature. HCl evolved immediately. After completion of the addition, the mixture was stirred magnetically for 1 h. Finally, a white solid material ASA was obtained (67 g) [27].

2.1.2. Preparation of 9-hexyl-9H-carbazole

In a dried 100 mL round bottom flask, carbazole (0.20 g, 1.1 mmol) was dissolved in DMSO (3 mL) followed by the addition of NaOH (0.40 g) and then drop wise addition of hexylbromide (0.33 g, 1.01 mmol). The reaction mixture was then heated at 90 °C overnight. Water was added to the reaction and the product isolated by filtration. The product was then washed thrice with 50 mL water, dried over Na₂SO₄ and concentrated. The pure product was obtained after silica gel column chromatography (n-Hexane) as a white solid [28].

White powder, yield: 85%, mp: 75–77 °C.

2.1.3. Typical procedure for the preparation of 9-Hexyl-9H-carbazole-3-carbaldehyde

In a dried 100 mL round bottom flask, Phosphorylchloride (1.55 mL, 1.25eq) was added drop wise to N,N-dimethylformamide (DMF, 0.88 mL, 1.15 eq) for 1 h at 0 °C. The mixture was stirred and N-(hexyl) carbazole (0.25 g, 1 mmol) added during 1 h at room temperature. After standing for 5 h at 90 °C, the mixture was poured into ice–water (30 mL), stirred 5 h, and neutralized with sodium hydroxide. The solution was extracted three times with ethyl acetate and dried with Na₂SO₄. The solvent was removed under reduced pressure. The residue was purified by silica gel column chromatography (eluent: ethyl acetate/n-hexane = 1:9).

Cream powder, Yield: 55%, mp: 70–74 °C.

IR (cm^{−1}): 3052, 2955, 2929, 2857, 2727, 1893, 1686, 1593, 1469, 1383, 1352, 1339, 1329, 1240, 1177, 1135, 807, 765, 748 and 730.

¹H NMR (400 MHz, DMSO-d₆) δ (ppm): 10.06 (s, 1H), 8.77 (s, 1H), 8.30 (d, *J* = 8 Hz, 1H), 7.79 (d, *J* = 8 Hz, 1H), 7.70 (m, 1H), 7.55 (m, 1H), 7.31 (t, *J* = 8 Hz, 1H), 4.46 (t, *J* = 8 Hz, 2H), 2.5 (DMSO-d₆), 1.77 (m, 2H), 1.25 (m, 6H) and 0.87 (t, *J* = 8 Hz, 3H).

¹³C NMR (100 MHz, DMSO-d₆) δ (ppm): 13.7, 22, 26, 28.4, 30.9, 38.9 (DMSO-d₆), 42.5, 109.7, 110.2, 120, 120.7, 122.11, 122.2, 124, 126.6, 126.7, 128.2, 140.4, 142.6 and 192.

2.1.4. Preparation of 4-Diphenylamino benzaldehyde

4-Diphenylamino-benzaldehyde was prepared by adopting literature procedure [29].

2.1.5. Typical procedure for the preparation of Bis (indolyl) methanes

In a dried 100 mL round bottom flask, A mixture of benzaldehyde (1 mmol), indole (2 mmol), and ASA (0.04 g) was stirred magnetically at 80 °C with ethanol, and the progress of the reaction was monitored by TLC. After completion of the reaction, in order to work up the product, catalyst was separated by filtration. Water was added and the product extracted into ethyl acetate. The organic layer was dried over anhydrous Na₂SO₄ and then evaporated under a vacuum to afford the crude product, which was further purified by column chromatography. In all the cases, the product obtained after the usual work up gave satisfactory spectral data.

Table 2

Thermodynamic data for the BIM1 and BIM2 in the gas phase calculated at DFT method by using 6-31G (d) basis set.

Compound	E ^a	H ^a	G ^a
BIM2	-1513.692399	-1513.691455	-1513.787688
BIM1	-1517.276455	-1517.275510	-1517.377393

^a Total energies in Hartree.

2.1.6. 3-[Bis-(1H-indol-3-yl)-methyl]-9-hexyl-9H-carbazole (BIM1)

Yield: 65%, solid, mp: 124–128 °C.

IR (cm⁻¹): 3423, 2925, 1590, 1483, 1415, 1198, 1120, 745.

¹H NMR (400 MHz, DMSO-d6) & (ppm): 8.34 (d, *J* = 1.2, 1H), 8.15 (d, *J* = 4, 1H), 8.07 (m, 2H), 7.7 (d, *J* = 8, 1H), 7.69 (d, *J* = 8, 1H), 7.55 (m, 4H), 7.48 (m, 2H), 7.17 (m, 4H), 6.87 (m, 2H), 6.70 (s, 2H), 4.49 (t, *J* = 8, 2H), 2.5 (DMSO-d6), 1.83 (m, 2H), 1.30 (m, 6H), 0.81 (t, *J* = 8, 3H).

¹³C NMR (100 MHz, DMSO-d6): 142.3, 141.0, 130.5, 130.4, 128.8, 126.8, 124.8, 122.8, 122.7, 121.3, 121.1, 120.8, 120.0, 116.5, 110.2, 109.9, 85.7, 43.0, 38.9(DMSO-d6), 31.4, 29.0, 26.6, 22.5, 14.3.

Mass: *m/z* 495 (M+1), 494, 465, 394, 363, 334, 245, 219, 173 and 130.

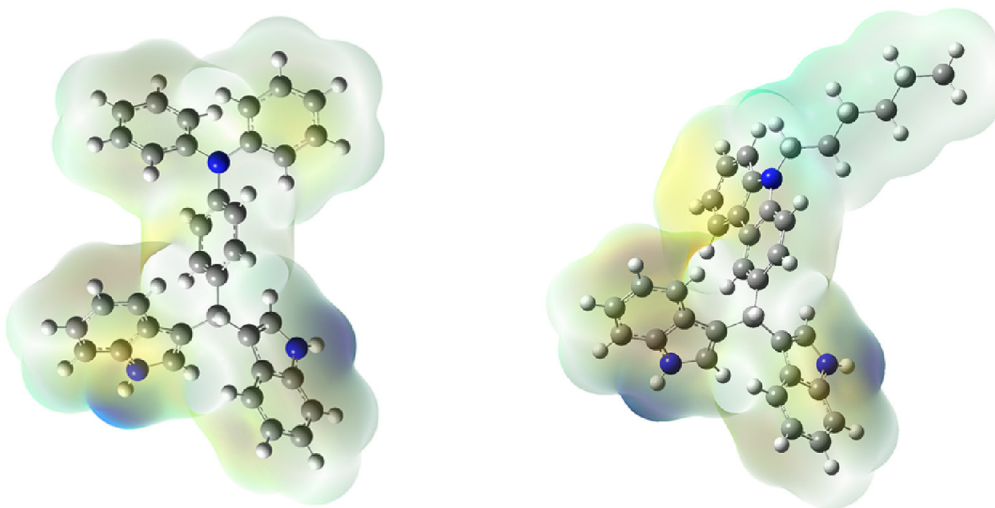


Fig. 2. Molecular electrostatic potential mapped on the isodensity surface of BIM1 and BIM2.

Table 3

Calculated and observed vibrational frequencies of BIM1 optimized by DFT method using 6-31G (d) basis set.

Entry	DFT	Exp.	Assignment
1	3670	3423	υ _{N40-H14, N39-H27}
2	3282		υ _{C8-H13, C24-H28}
3	3210, 3201, 3189, 3181		υ _{C44-H47, C46-H50, C45-H49, C48-H51}
4	3208, 3198, 3178, 3278		υ _{C3-H9, C4-H10, C5-H11, C6-H12}
5	3208, 3198		υ _{C16-H41, C18-H22, C21-H25, C23-H26}
6	3201, 3196		υ _{C30-H33, C31-H35, C34-H37}
7	3186, 3186		υ _{C16-H41, C18-H22, C23-H26, υ C3-H9, C5-H11, C6-H12}
8	3181		υ _{C44-H47, C45-H49,C46-H50, C48-H51}
9	3178		υ _{C3-H9, C4-H10, C5-H11, C6-H12}
10	3178		υ _{C16-H41, C18-H22, C21-H25, C23-H26}
11	3178		υ _{C31-H35, C34-H37}
12	3112		υ _{C65-H68, H69, H70}
13	3107, 3043, 3041		υ _{C65-H69, H70, C64-H66, H67}
14	3103, 3078, 3067, 3057		υ _{C52-H54,H58, C53-H57, H58}
15	3028, 3017, 3012		υ _{C56-H60, H61,C64-H66, H67, C59-H62,H63}
16	2987	2925	υ _{C15-H71}
17	1678, 1655		υ _{Carbazole Ring}
18	1676, 1677, 1634	1590	υ _{indole Ring}
19	1544, 1537, 1528, 1339	1483	δ _{C52-H54,C52-H55, C53-H57, C53-H58, C56-H60, C56-H61, C59-H62, C59-63, C64-H67,C64-H66, C65-H68, C65-H69, C65-H70}
20	1348	1415	δ _{Ring Carbazole}
21	1333, 1328		δ _{Ring 1,2,3,4}
22	1247		δ _{C15-H71, C16-H41, C18-H22, C21-H25, C23-H26, C24-H28}
23	1186	1198	δ _{H Ring 1,3}
24	1044	1120	Ring def. 2
25	1043		Ring def. 3
26	965		τ _{C16-H41, C18-H22, C21-H25, C23-H26}
27	964		τ _{C16-H41, C18-H22, C3-H9, C4-H10, C5-H11, C6-H12}
28	964		τ _{C44-H47, C45-H49, C46-H50, C48-H51}
29	935		τ _{C31-H35, C34-H37}
30	890, 889		rings def. 1,2,3,4
31	759	745	τ _{Carbazole Ring}

2.1.7. {4-[Bis-(1H-indol-3-yl)-methyl]-phenyl}-diphenyl-amine (BIM2)

Yield: 85%; solid, mp: 169–172 °C.

IR (cm^{-1}): 3412, 3054, 2924, 2855, 2213, 1708, 1586, 1504, 1490, 1456, 1414, 1334, 1092, 112, 853, 790, 742.

^1H NMR (400 MHz, DMSO-*d*6) & (ppm): 7.36 (d, *J* = 8, 2H), 7.31 (m, 4H), 7.24 (t, *J* = 4, 4H), 7.04 (t, *J* = 8, 4H), 6.99 (m, 2H), 6.96 (d, *J* = 8, 4H), 6.94 (m, 2H), 6.92 (s, 1H), 6.88 (m, 4H), 2.5(DMSO-*d*6).

^{13}C NMR (100 MHz, DMSO-*d*6:3.9): 147.8, 145.3, 140.4, 137.0, 131.1, 130.5, 129.9, 129.8, 127.1, 127.0, 124.4, 123.9, 123.7, 122.9, 121.3, 119.5, 118.6, 111.9, 38.9(DMSO-*d*6).

Mass: *m/z* 490 (M+1), 489, 388, 274, 245, 203, 117 and 77.

3. Computational details

Theoretical calculations were performed using GAUSSIAN 98 package and the Gauss-View molecular visualization program [30]. The geometries of (BIM1) and (BIM2) were optimized by using the B3LYP method with the 6-31G (d) basis set.

4. Results and discussion

4.1. Synthesis

The molecular structures and synthetic routes of the (BIM1) and (BIM2) are represented in Schemes 1 and 2 respectively. Both of the Bis (indolyl) methans have been synthesized by the stepwise synthetic protocol. Every Bis (indolyl) methans contains two essential parts include aldehyde and indoles. 9-Hexyl-9H-carbazole-3-carbaldehyde and 4-diphenylaminobenzaldehyde have been

selected as aromatic aldehyde. In order the synthesis of (BIM1) n the first step; hexyl was introduced to carbazole in the presences of NaOH and DMSO as solvent. In the next step 9-hexyl-9H-carbazole undergoes Vilsmeier–Haack reaction for formylation. Also triphenylamine undergoes Vilsmeier–Haack reaction for formylation. In final synthetic protocol indole in the presence of alumina sulphuric acid (ASA) (10% mol), ethanol, aromatic aldehydes were used for preparation of Bis (indolyl) methans.

4.2. Geometry optimization and energies

The optimized molecular structure of Bis (indolyl) methans along with numbering of atoms are shown in Fig. 1. The optimized geometrical parameters of Bis (indolyl) methans obtained by DFT-B3LYP/6-31G (d) are listed in Table 1. Comparison of the theoretical bond lengths of two Bis (indolyl) methans indicates that all bond length around C15 are equal roughly. These bonds include C7-C8, C15-C20, C20-C24, C15-H65, C15-H71 and calculated bond lengths at DFT/B3LYP level are 1.4452, 1.5172, 1.3724 and 1.1016 Å, respectively.

In addition, we investigated the bond angles of Bis (indolyl) methane molecules.

4.3. Thermodynamic properties

The dependence of Bis (indolyl) methanes thermodynamic properties on the C15 substitutions was investigated. Thermodynamic data for the BIM1 and BIM2 in the gas phase calculated at DFT method by using 6-31G (d) basis set. Result are presented in Table 2. It indicate all parameter E, H and G for BIM1 is higher in

Table 4

Calculated and observed vibrational frequencies of BIM2 optimized by DFT method using 6-31G (d) basis set.

Entry	DFT	Exp.	Assignment
1	3670	3412	ν N62-H27, N63-H14
2	3670		ν N63-H14
3	3283, 3283		ν C8-H13, C24-H28
4	3218, 3191		ν C41-H44, C42-H46, C43-H48, C45-H49, C47-H49
5	3218, 3190		ν C52-H55, C53-H57, C54-H59, C56-H60, C58-H61
6	3215,3215, 3206		ν C52-H55, C53-H57, C54-H59, C56-H60, C58-H61
7	3214, 3212		ν C32-H37, C30-H33, C31-H35, C34-H38
8	3209, 3188, 3179		ν C16-H64, C18-H22, C21-H25, C23-H26
9	3208, 3198, 3186		ν C3-H9, C4-H10, C5-H11, C6-H12
10	3199	3054	ν C16-H54, C18-H22, C21-H25, C23-H26
11	3196	2924	ν C30-H33, C32-H37
12	2987	2855	ν C15-H65
13	1677, 1677, 1634	2213	ν Ring 1,2,3,4
14	1669, 1657	1708	ν Ring 5,6,7
15	1466	1586	δ_H Ring 5
14	1461, 1459	1504	ν N63-H12, N62-H27
15	1394	1490	ν C15-H65, C15-C20, C20-C17, C20-C24
16	1388	1456	Ring def. 1,2
17	1385	1414	Ring def. 3,4
18	1372		δ_H Ring 6,7
19	1359	1335	δ_H Ring 1,2,3,4,5
20	1358		Ring def. 5,6
21	1358		Ring def. 5,6,7
22	1147		δ_H Ring 5
23	1037	1092	Twisting Ring 5
24	1016	1011	Twisting Ring 6,7
25	987		γ Ring 6
26	972		γ Ring 5
27	966		γ Ring 3
28	965	853	γ Ring 1
29	783	790	τ Ring 1,2
30	777		τ Ring 3,4
31	772		τ Ring 6,7
32	737	742	τ Ring 5
33	207		Twisting

Table 5

Proton	B3LYP/6-31G(d)	Exp.	Carbon	B3LYP/6-31G(d)	Exp.
H9	6.65	7.55	C1	113.32	126.8
H10	6.65	7.55	C2	120.54	130.4
H11	6.52	7.17	C3	110.26	122.7
H12	7.00	7.70	C4	108.46	121
H13	6.02	6.87	C5	105.99	110.2
H14	6.19	7.17	C6	106.64	116.5
H22	6.65	7.48	C7	107.97	120.0
H25	6.65	7.48	C8	110.26	122.7
H26	6.65	7.55	C15	35.16	85.7
H27	6.13	6.87	C16	107.06	120.0
H28	5.71	6.70	C17	113.35	126.8
H33	7.51	8.34	C18	105.97	110.2
H35	7.20	8.15	C19	120.22	130.4
H37	6.82	7.55	C20	120.54	130.4
H41	7.07	7.69	C21	108.41	120.8
H47	6.65	7.17	C23	95.87	109.9
H49	7.37	8.07	C24	110.26	122.7
H50	6.91	8.07	C29	122.5	130.5
H51	6.65	7.17	C30	108.00	120.8
H54	3.75	4.49	C31	114.25	128
H55	3.75	4.49	C32	110.66	122.8
H57	1.57	1.83	C34	94.35	109.9
H58	1.57	1.83	C36	124.55	141.0
H60	1.26	1.30	C42	125.60	142.3
H61	1.26	1.30	C43	110.33	122.8
H62	1.15	1.30	C44	94.04	109.9
H63	1.15	1.30	C45	107.27	120.0
H66	1.26	1.30	C46	111.46	124.8
H67	1.26	1.30	C48	105.50	110.2
H68	0.87	0.81	C52	36.67	43
H69	0.67	0.81	C53	24.12	29
H70	0.67	0.81	C56	23.20	22.6
H71	5.71	6.70	C59	26.94	31.4
—			C64	19.06	22.5
—			C65	8.78	14.30

comparison to other Bis (indolyl) methanes. The E value is -1517.276455 and -1513.692399 for BIM1 and BIM2 respectively.

4.4. Molecular electrostatic potential

Electrostatic potential maps, also known as electrostatic potential energy maps, or molecular electrical potential surfaces, illustrate the charge distributions of molecules three dimensionally. These maps allow us to visualize variably charged regions of a molecule. Knowledge of the charge distributions can be used to determine how molecules interact with one another. In order to understand the roles of the different groups substituted at the C15-position by manipulation of the heterocyclic ring, we compared the respective molecular electrostatic potential maps derived by molecular orbital calculations. Potential increases in the order blue > green > yellow > orange > red. Electrostatic potential maps of BIM1 and BIM2 are presented in Fig. 2. The positive (blue color) were related to nucleophilic reactivity. It shows that the positive regions are mainly over NH groups in indole rings. It indicates the both molecules have nucleophilic reactivity mainly and substituted groups in C15 do not differ charge distributions significantly.

4.5. Assignments of vibrational frequencies

One of the most useful tool for the identification of functional groups of organic compounds, studies on molecular conformation and reaction kinetics is application of vibrational spectroscopy. The vibrational frequencies and also approximate description of each normal vibrational mode obtained using DFT/B3LYP method with 6-31G (d) basis set are given in Tables 3 and 4. The observed band

Table 6

Proton	B3LYP/6-31G(d)	Exp.	Carbon	B3LYP/6-31G(d)	Exp.
H9	6.65	6.99	C1	113.13	127.1
H10	6.65	6.97	C2	120.40	137.0
H11	6.65	6.97	C3	95.95	111.9
H12	7.07	7.36	C4	108.55	121.3
H13	5.88	6.88	C5	106.10	118.2
H14	6.12	6.88	C6	106.65	118.2
H22	6.65	6.97	C7	107.27	119.2
H25	6.65	6.97	C8	109.90	122.9
H26	6.65	6.99	C15	34.96	85.7
H27	6.21	6.88	C16	107.14	119.2
H28	5.88	6.88	C17	113.17	129.8
H33	6.65	7.36	C18	106.13	118.2
H35	7.00	7.36	C19	120.18	137.0
H37	6.47	6.96	C21	108.57	121.3
H38	6.65	6.96	C23	95.98	111.9
H44	6.65	7.24	C24	109.71	122.9
H46	6.47	7.04	C29	125.78	140.4
H48	6.65	7.31	C30	116.38	131.1
H49	6.65	7.31	C31	116.90	131.1
H50	6.41	6.94	C33	111.28	124.4
H55	6.65	7.24	C34	111.65	127
H57	6.65	7.04	C36	132.55	145.3
H59	6.65	7.31	C40	134.09	147.8
H60	6.65	7.31	C41	110.46	123.7
H61	6.47	6.94	C42	110.93	123.9
H64	7.00	7.36	C43	115.00	129.9
H65	5.43	6.92	C45	115.33	130.5
—			C47	108.14	121.3
—			C51	134.35	147.8
—			C52	110.95	123.9
—			C53	110.86	123.7
—			C54	115.30	130.5
—			C56	115.09	129.9
—			C58	108.24	121.3

frequencies in the infrared spectrum of compound are compared by the experimental frequencies in Tables 3 and 4

4.5.1. N-H vibrations

In all the heterocyclic compounds, the NH stretching vibrations occur in the region $3500\text{--}3000\text{ cm}^{-1}$ [31]. The N-H stretching vibration is calculated to be $3669\text{--}70\text{ cm}^{-1}$ and observed as high intense peak at $3412\text{--}23\text{ cm}^{-1}$ in the IR spectrum.

4.5.2. C-H vibrations

C-H stretching frequencies appear in the range of $3100\text{--}3000\text{ cm}^{-1}$ in aromatic compound and in the range of $2850\text{--}3000\text{ cm}^{-1}$ in aliphatic. The observed frequency value 3053 cm^{-1} (aromatic units) and $2855\text{--}2924\text{ cm}^{-1}$ (C15-H) are in agreement with values in the range of $3282\text{--}3012$ and 2938 cm^{-1} (B3LYP/6-31G (d) method). Also C-H stretching frequencies of hexyl moiety observed in the range of $3012\text{--}3112\text{ cm}^{-1}$. The theoretically calculated vibrations corresponding to C-H stretch show good agreement with the experimentally observed vibrations.

4.5.3. C-C vibrations

The bands between 1620 and 1680 cm^{-1} and $1500\text{--}1700$ in aromatic compounds are usually assigned to C=C stretching and bending frequencies respectively. The C=C stretching vibrations of the Bis (indolyl) methanes are found in the range of $1707\text{--}2212\text{ cm}^{-1}$ in FT-IR for BIM1 and 1590 cm^{-1} for BIM2. DFT predict values in the range of $1657\text{--}1677$ and $1633\text{--}1678\text{ cm}^{-1}$ for title compounds respectively. Also in-plane bending vibration observed around 1414 and 1335 for BIM1 and BIM2 respectively. Theoretical results predict values in the range of $1327\text{--}1466\text{ cm}^{-1}$.

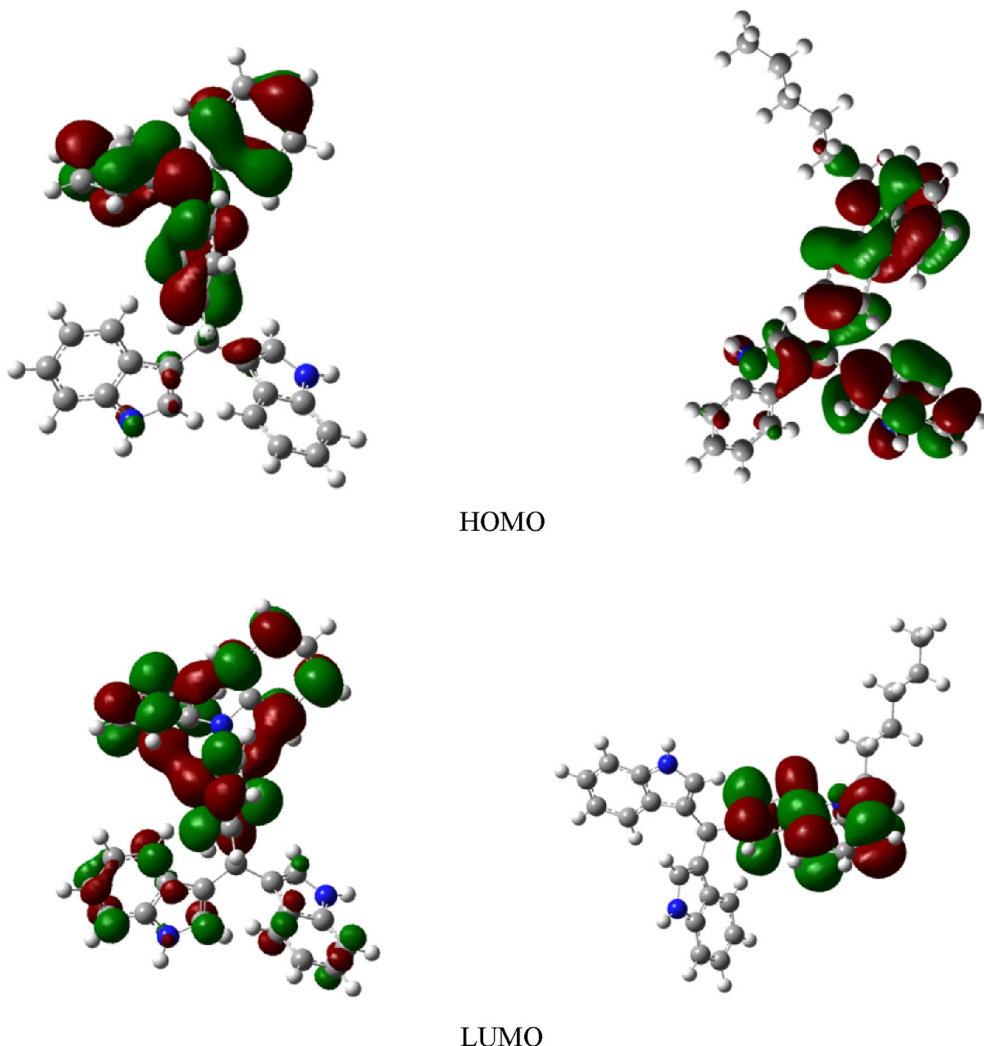


Fig. 3. Patterns of the principle highest occupied and lowest unoccupied molecular orbitals of BIM1 and BIM2 obtained with DFT/6-31 G (d) method.

Table 7

Some of the calculated energy values of BIM1 and BIM2 in their ground state with singlet symmetry.

Compound	HOMO (a.u.)	LUMO (a.u.)	HOMO-LUMO gap, ΔE (a.u.)
BIM2	-0.17812	-0.00956	0.16856
BIM1	-0.18704	-0.02109	0.16595

for in-plane bending vibrations. The theoretically computed frequencies using B3LYP/6-31 G (d) method are assigned for C–C and C=C stretching vibrations approximately coincides with FT-IR.

4.6. NMR spectra

The GIAO method is one of the most common approaches for calculating isotropic nuclear magnetic shielding tensors. GIAO ^{13}C NMR and ^1H NMR chemical shifts calculations of the title compounds were carried out by using B3LYP/functional with 6-31G (d) basis set. Chemical shifts were reported in parts per million relative to TMS for ^1H and ^{13}C NMR spectra. Experimental and calculated ^1H NMR and ^{13}C NMR chemical shifts (ppm) of BIM1 and BIM2 are presented in Tables 5 and 6.

Compound BIM1: The studied molecule has 17 hydrogen atoms in the aromatic ring and 14 hydrogen atoms in aliphatic parts. 29

hydrogen atoms attached to the carbon atom and 2 hydrogen atom attached to the nitrogen atoms. In the ^1H NMR spectra just one of aliphatic protons appears at 6.7 ppm as a singlet, because of H71 is connected to four aromatic rings. The chemical shift value of H71 has been observed at 5.71 ppm at DFT method. The chemical shift value for all aromatic hydrogen has been observed around 6.82–8.24 and 6.13–7.51 ppm experimentally and at DFT method respectively. Also all aliphatic hydrogens show chemical shift around 0.81–4.49 and 0.67–3.27. As shown in Fig. 1, the studied molecule has 35 different carbon atoms, which is consistent with the structure based on molecular symmetry. The chemical shift value of C15 which is in bonded to four aromatic rings have been observed at 85.7 and 35.16 ppm experimentally and at DFT/6-31G(d) respectively. The experimental and theoretical values obtained around 14.30–43 and 8.78–36.67 ppm respectively for other aliphatic carbons. The agreement between the experimental and calculated data is satisfactory.

Compound BIM2: This molecule has 26 hydrogen atoms in the aromatic ring and one aliphatic hydrogen atom. 25 hydrogen atoms attached to the carbon atom and 2 hydrogen atoms attached to the nitrogen atoms. In the ^1H NMR spectra just one of aliphatic protons appears at 6.92 ppm as a singlet, because of H65 is bonded to three aromatic rings. The chemical shift value of H65 has been observed at 5.43 ppm at DFT method. The chemical shift value for all

Table 8

Calculated NBO charges on atoms of Bis (indolyl) methanes in the gas phase.

Atom no.	BIM1	Atom no.	BIM2
C1	-0.087	C1	-0.088
C2	0.159	C2	0.159
C3	-0.268	C3	-0.267
C4	-0.249	C4	-0.240
C5	-0.258	C5	-0.258
C6	-0.249	C6	-0.215
C7	-0.106	C7	-0.107
C8	-0.023	C8	-0.022
C15	-0.279	C15	-0.281
C16	-0.216	C16	-0.216
C17	-0.091	C17	-0.092
C18	-0.259	C18	-0.259
C19	0.157	C19	0.157
C20	-0.162	C21	-0.240
C21	-0.241	C23	-0.269
C23	-0.248	C24	-0.022
C29	-0.050	C29	-0.037
C30	-0.199	C30	-0.221
C31	-0.216	C31	-0.218
C32	-0.077	C32	-0.245
C34	-0.272	C34	-0.245
C36	0.118	C36	0.143
C42	0.185	C40	0.159
C43	-0.082	C41	-0.246
C44	-0.279	C42	-0.251
C45	-0.202	C43	-0.226
C46	-0.226	C45	-0.224
C48	-0.263	C47	-0.252
C52	-0.245	C51	0.151
C53	-0.462	C52	-0.252
C56	-0.455	C53	-0.252
C59	-0.451	C54	-0.225
C64	-0.452	C56	-0.226
C65	-0.673	C58	-0.252
H9	0.232	H9	0.232
H10	0.233	H10	0.234
H11	0.233	H11	0.233
H12	0.287	H12	0.237
H13	0.243	H13	0.243
H14	0.428	H14	0.429
H22	0.233	H22	0.234
H25	0.233	H25	0.234
H26	0.232	H26	0.232
H27	0.428	H27	0.429
H28	0.243	H28	0.242
H33	0.244	H33	0.245
H35	0.235	H35	0.236
H37	0.234	H37	0.247
H41	0.248	H38	0.247
H47	0.234	H44	0.246
H49	0.236	H46	0.246
H50	0.235	H48	0.236
H51	0.235	H49	0.248
H54	0.237	H50	0.235
H55	0.236	H55	0.247
H57	0.235	H57	0.244
H58	0.136	H59	0.237
H60	0.226	H61	0.235
H61	0.226	H64	0.241
H62	0.226	H65	0.263
H63	0.226	H68	0.235
H66	0.226	N39	-0.447
H67	0.226	N62	-0.561
H68	0.232	N63	-0.560
H69	0.255	—	—
H70	0.255	—	—
H71	0.262	—	—
N38	-0.391	—	—
N39	-0.561	—	—
N40	-0.561	—	—

aromatic hydrogen has been observed in the range of 6.88–7.36 and 5.88–7.07 ppm experimentally and at DFT method respectively. As shown in Fig. 1, the studied molecule has 35 different

carbon atoms, which is consistent with the structure based on molecular symmetry. The chemical shift value of C15 which is in bonded to three aromatic rings have been observed at 85.7 and 34.96 ppm experimentally and at DFT respectively, using 6-31G(d) basis set. Similar to previous compound the experimental and theoretical values for aromatic carbons of BIM2 is in the range of 95.5–134.35 and 111.9–147.8 ppm respectively. Also the agreement between the experimental and calculated data is satisfactory.

4.7. HOMO and LUMO analyses

On the base of frontier molecular orbital theory, HOMO and LUMO are acronyms for highest occupied molecular orbital and lowest unoccupied molecular orbital, respectively. The energy difference between the HOMO and LUMO is termed the HOMO–LUMO gap. HOMO and LUMO are sometimes referred to as frontier orbitals. The gap between the HOMO and LUMO energy levels of the molecule is a tool for reactivity determination of the molecule. As it decreases, the reactivity of the molecule increases leading to a decrease in the stability of the molecule. The atomic orbital compositions of the Frontier molecular orbital are shown in Fig. 3. In BIM2 molecule, the π nature is delocalized over the whole triphenyl amine rings and indole rings slightly and the HOMO is located over just triphenyl amine rings. For 3 BIM1, In the HOMO, the charge density is mainly accumulated on the carbazole and some part of indole rings and LUMO more charge density moves to carbazole rings.

The HOMO–LUMO energy gap of Bis (indolyl) methans is calculated at B3LYP/6-31G levels and are shown in Table 7. HOMO–LUMO energy gap explains the eventual charge transfer interaction within the molecule, which influences the biological activity of the molecule. Molecular orbital theory, HOMO and LUMO can elucidate bioactivity of compounds. The interaction between these molecules and the receptor of bacteria is dominated by π – π interaction among these frontier molecular orbitals [20]. Therefore it is predicted that in In BIM2, all triphenyl amine and partially parts of indole rings participate in bioactivity of compounds. BIM1 showed different participation; both carbazole and indole rings have significant effect.

4.8. NBO analyses

NBO is a calculated bonding orbital with maximum electron density. Natural (localized) orbitals are used in to calculate the distribution of electron density in atoms and in bonds between atoms. Therefore NBO calculations can provide the detailed insight into the electronic structure of molecule. They have the “maximum-occupancy character” in localized 1-center and 2-center regions of the molecule. Natural bond orbital analyses provides an efficient method for determination of electron donor orbital, acceptor orbital and the interacting stabilization energy resulted from the second-order micro-disturbance theory. NBO analysis has been performed on the Bis (indolyl) methans at the B3LYP/6-31G (d) level in order to elucidate, the intra-molecular rehybridization and delocalization of electron density within the molecules. The calculated value of NBO charges using natural population analysis (NPA) of optimized structures of Bis (indolyl) methans are given in Table 8. It can be seen that, in BIM1, C65 and N40 and in BIM2, N62 and N63 have the most negative charges.

Compound BIM1: The magnitudes of charge on carbon atoms are changing between -0.673 and 0.185 at the B3LYP/6-31G (d) level. This molecule has some carbons, which binding to nitrogen atoms and these carbons have positive charge. In this molecule there are three nitrogen atoms that have negative charge, the charge values for N38, N39 and N40 are -0.391, -0.561 and -0.561

at B3LYP/6-31G (d) level of calculation, respectively. The magnitudes of the hydrogen atomic charges are found to be positive at the basis sets. The magnitude of the hydrogen atomic charges are arranged in an order from 0.136 to 0.428 at B3LYP/6-31G (d) method. The two hydrogen atoms, H14 and H27 which have binding to nitrogen have more positive charge than other hydrogen atoms. H14 and H27 hydrogens bonded to atoms with same electronegativity. Therefore charge value for these atoms is equal. The charge values for H14 and H27 are 0.428 at B3LYP/6-31G (d) level of calculation, respectively.

Compound BIM2:

5. Conclusions

In the present work, we have synthesized and calculated the thermodynamic properties, geometric parameters, vibrational frequencies, ^{13}C and ^1H NMR chemical shifts, Molecular electrostatic potential, HOMO-LUMO levels and NBO analysis of the two novel Bis (indolyl) methanes derivatives BIM1 and BIM2 by using B3LYP method with 6-31G (d) basis set. The calculated vibrational modes assigned to their experimental values. It has been observed that all scaled frequencies are in good agreement with experimental values. The effect of substituents new aldehydes has been studied to the variation of charge distribution in the molecule, and consequently affects the structural, electronic and vibrational parameters. HOMO and LUMO analyses revealed these compounds may have bioactivity due to $\pi-\pi$ interaction in all triphenyl amine and partially parts of indole rings of BIM2 and carbazole and indole rings in BIM1. NBO calculation indicates in BIM1, C65 and N40 and in BIM2, N62 and N63 have the most negative charges.

Acknowledgement

The authors express their appreciation to the Graduate School and Research Council of the Yasouj University for financial support of this work.

Abbreviations

ASA	Alumina Sulfuric Acid
BIM2	{4-[Bis-(1H-indol-3-yl)-methyl]-phenyl}-diphenyl-amine
BIM1	3-[Bis-(1H-indol-3-yl)-methyl]-9-hexyl-9H-carbazole
DFT	Density Functional Theory
DMSO	Dimethyl Sulfoxide
HOMO	Highest Occupied Molecular Orbital
LUMO	Lowest Unoccupied Molecular Orbital
GIAO	Gauge Invariant Atomic Orbital
NBO	Natural Bond Orbital
NMR	Nuclear Magnetic Resonance
TLC	Thin layer Chromatography

References

- [1] F. Lingens, W. Goebel, biosynthese des tryptophans in *Saccharomyces cerevisiae* II. Über die konstitution unbekannter akkumulate bei trp-mutanten, *Biochem. Biophys. Acta Gen. Subj.* 148 (1967) 70–83.
- [2] J.K. Porter, C.W. Bacon, J.D. Robbing, D.S. Himmelsbach, H.C. Higman, Indole alkaloids from *Balanisia epichloe* (Weese), *J. Agric. Food Chem.* 25 (1977) 88–93.
- [3] E. Fahy, B.C.M. Potts, D.J. Faulkner, K. Smith, 6-Bromotryptamine derivatives from the Gulf of California Tunicate *Didemnum candidum*, *J. Nat. Prod.* 54 (1991) 564–569.
- [4] C. Hong, G.L. Firestone, L.F. Bjeldanes, Bcl-2 family-mediated apoptotic effects of 3, 3'-diindolylmethane (DIM) in human breast cancer cells, *Biochem. Pharmacol.* 63 (2002) 1085–1097.
- [5] X. Ge, S. Yannai, G. Rennert, N. Gruener, F.A. Fares, 3,3'-Diindolylmethane induces Apoptosis in human cancer cells, *Biochem. Biophys. Res. Commun.* 228 (1996) 153–158.
- [6] X. He, S. Hu, K. Liu, Y. Guo, J. Xu, S. Shao, Oxidized Bis(indolyl)methane: a simple and efficient chromogenic-sensing molecule based on the proton transfer signaling, *Mode Org. Lett.* 8 (2006) 333–336.
- [7] W.A. Remers, in: W.J. Houlihan (Ed.), *Heterocyclic Compounds*, Interscience Publishers, New York, 1972, p. 1.
- [8] A. Maiti, P. Bhattacharya, Montmorillonite clay-catalysed synthesis of Bis (indol-3-yl)-methanes and 1, 2-Bis (indol-3-yl) ethanes, *J. Chem. Res.* 11 (1997) 424–425.
- [9] M. Rekha, H.R. Manjunath, N. Nagaraju, Mn/Al₂O₃ and Mn/ZrO₂ as selective catalysts for the synthesis of bis (indolyl) methanes: the role of surface acidity and particle morphology, *J. Ind. Eng. Chem.* 19 (2013) 337–346.
- [10] M.A. Zolfogil, P. Salehi, M. Shiri, A. Sayadi, A. Abdoli, H. Keypour, M. Rezaeivala, K. Niknam, E. Kolvari, A simple and efficient route for the synthesis of di and tri(bis(indolyl) methanes) as new triarylmethanes, *Mol. Divers.* 12 (2008) 203–207.
- [11] J.-T. Li, M.-X. Sun, G.-Y. He, X.-Y. Xu, Efficient and green synthesis of bis(indolyl)methanes catalyzed by ABS in aqueous media under ultrasound irradiation, *Ultrasound. Sonochem.* 18 (2011) 412–414.
- [12] S. Khaksar, S.M. Ostad, Pentafluorophenylammonium triflate as an efficient, environmentally friendly and novel organocatalyst for synthesis of bis-indolyl methane derivatives, *J. Fluor. Chem.* 132 (2011) 937–939.
- [13] Z. Xiang, Z. Liu, X. Chen, Q. Wu, X. Lin, Biocatalysts for cascade reaction: porcine pancreas lipase (PPL)-catalyzed synthesis of bis(indolyl)alkanes, *J. Amino Acids* 45 (2013) 937–945.
- [14] F. Shirini, N. Ghaffari Khaligh, O. Goli Jolodar, An efficient and practical synthesis of bis(indolyl)methanes catalyzed by N-sulfonic acid poly(4-vinylpyridinium) chloride, *Dyes Pigments* 98 (2013) 290–296.
- [15] A. Khalafli-Nezhad, A. Parhami, A. Zare, A.R. Moosavi Zare, A. Hasaninejad, F. Panahi, Trityl chloride as a novel and efficient organic catalyst for room temperature preparation of Bis(indolyl)methanes under solvent-free conditions in neutral media, *Synthesis* 4 (2008) 617–621.
- [16] P. Pratim Kaishap, C. Dohutia, Synthetic approaches for Bis (indolyl) methanes, *I. J.P.S.R.* 4 (2013) 1312–1322.
- [17] A. Panitsiri, S. Tongkhan, W. Radchatawedchakoon, U. Sakee, Synthesis and anion recognition studies of novel bis (4-hydroxycoumarin) methane azo dyes, *J. Mol. Struct.* 1107 (2016) 14–18.
- [18] S. Eryilmaz, M. Güll, E. İnkaya, M. Taş, Isoxazole derivatives of alpha-pinene isomers: synthesis, crystal structure, spectroscopic characterization (FT-IR/NMR/GC-MS) and DFT studies, *J. Mol. Struct.* 1108 (2016) 209–222.
- [19] J.L. Naika, B. Venkatram Reddy, N. Prabavathi, Experimental (FTIR and FT-Raman) and theoretical investigation of some pyridine-dicarboxylic acids, *J. Mol. Struct.* 1100 (2015) 43–58.
- [20] G.S. Suresh Kumar, A. Antony Muthu Prabu, S. Jegan Jenniefer, N. Bhuvanesh, P. Thomas Muthiah, S. Kumaresan, Syntheses of phenoxyalkyl esters of 3,30-bis(indolyl)methanes and studies on their molecular properties from single crystal XRD and DFT techniques, *J. Mol. Struct.* 1047 (2013) 109.
- [21] S.Y. Ebrahimipour, H. Khabazadeh, J. Castro, I. Sheikholeslami, A. Crochet, M. Katharina, Fromm, *cis*-Dioxido-molybdenum(VI) complexes of tridentate ONO hydrazone Schiff base: Synthesis, characterization, X-ray crystal structure, DFT calculation and catalytic activity, *Inorg. Chim. Acta* 427 (2015) 52–61.
- [22] A.S. Salimi Beni, A.N. Chermahini, H. Sharghi, S.M. Monfared, MP2, DFT and ab initio calculations on thioxanthone, *Spectrochim. Acta A* 82 (2011) 49–55.
- [23] A. Salimi Beni, S. Mirzaei Monfared, DFT and MP2 calculations on new series of hydroxythioxanthones, *J. Mol. Struct.* 1039 (2013) 8–21.
- [24] A. Salimi Beni, Z. Dalirnasab, A. Teimouri, A. Najafi Chermahini, Studies on tautomerism in the triazoline dione, *Can. J. Chem.* 89 (2011) 1387–1395.
- [25] N. Wang, X. Liang, Q. Li, Y. Liaoab, S. Shao, Nitro-substituted 3,3'-bis(indolyl) methane-modified silica gel as a sorbent for solid-phase extraction of flavonoids, *RSC Adv.* 5 (2015) 15500–15506.
- [26] P. Praveen, P.S. Parameswaran, M.S. Majik, Bis(indolyl)methane alkaloids: Isolation, bioactivity, and syntheses, *Synthesis* 47 (2015) 1827–1837.
- [27] S. Besoluk, M. Kucukislamoglu, M. Nebioglu, M. Zengin, M. Arslan, Solvent-free synthesis of dihydropyrimidinones catalyzed by alumina sulfuric acid at room temperature, *J. Iran. Chem. Soc.* 5 (2008) 62–66.
- [28] A. Salimi Benia, M. Zarandia, A.R. Madram, Y. Bayat, A. Najafi Chermahini, R. Ghahary, Synthesis and characterization of organic dyes bearing new electron-withdrawing group for dye-sensitized solar cells, *Electrochim. Acta* 186 (2015) 504–511.
- [29] M. Behl, E. Hattemer, M. Brehmer, R. Zentel, Tailored semiconducting polymers: living radical polymerization and NLO-Functionalization of triphenylamines, *Macromol. Chem. Phys.* 203 (2002) 503–510.
- [30] M.-J. Frisch, et al., GAUSSIAN 98, Revision A.11, Gaussian Inc., Pittsburgh, PA, 1998.
- [31] B. Datt Joshi, A. Srivastava, P. Tandon, S. Jain, Molecular structure, vibrational spectra and HOMO, LUMO analysis of yohimbine hydrochloride by density functional theory and ab initio Hartree–Fock calculations, *Spectrochim. Acta A* 82 (2011) 270–278.